JVI Journals.ASM.org

Identification of Virulence Determinants within the L Genomic Segment of the Pichinde Arenavirus

Lisa McLay,[a] Shuiyun Lan,[a] Aftab Ansari,[a] Yuying Liang,[b] Hinh Ly[a,b]

Department of Pathology and Laboratory Medicine, Emory University, Atlanta, Georgia, USA[a]; Department of Veterinary and Biomedical Sciences, University of Minnesota, Twin Cities, Minnesota, USA[b]

Several arenaviruses are responsible for causing viral hemorrhagic fevers (VHF) in humans. Lassa virus (LASV), the causative agent of Lassa fever, is a biosafety level 4 (BSL4) pathogen that requires handling in BSL4 facilities. In contrast, the Pichinde arenavirus (PICV) is a BSL2 pathogen that can cause hemorrhagic fever-like symptoms in guinea pigs that resemble those observed in human Lassa fever. Comparative sequence analysis of the avirulent P2 strain of PICV and the virulent P18 strain shows a high degree of sequence homology in the bisegmented genome between the two strains despite the polarized clinical outcomes noted for the infected animals. Using reverse genetics systems that we have recently developed, we have mapped the sequence changes in the large (L) segment of the PICV genome that are responsible for the heightened virulence phenotype of the P18 strain. By monitoring the degree of disease severity and lethality caused by the different mutant viruses, we have identified specific residues located within the viral L polymerase gene encoded on the L segment essential for mediating disease pathogenesis. Through quantitative reverse transcription-PCR (RT-PCR) analysis, we have confirmed that the same set of residues is responsible for the increased viral replicative potential of the P18 strain and its heightened disease severity *in vivo*. Our laboratory findings serve to reinforce field observations that a high level of viremia often correlates with severe disease outcomes in LASV-infected patients.

Arenaviruses are enveloped, ambisense RNA viruses that have a single-stranded genome which is composed of a large (L) segment of ~7.2 kb and a small (S) segment of ~3.4 kb (1). The S segment encodes the glycoprotein (GPC) in the positive sense and nucleoprotein (NP) in the negative sense, whereas the L segment encodes the Z matrix protein in the positive orientation and the L polymerase in the negative orientation (1). Each segment contains highly structured intergenic regions (IGRs) located between the two open reading frames. These are thought to be involved in transcriptional termination (1, 2). Additionally, the distal 19 nucleotides of the viral genomic segments are imperfectly complementary to each other and are presumed to form panhandle structures, thereby circularizing the genome (3–5). These panhandles are also thought to form an attachment point for the L polymerase, which together with NP mediates both viral genome replication and mRNA transcription (3, 6–8). NP has also been shown to mediate type I interferon (IFN) suppression in response to viral infection (9–12).

Several arenaviruses are responsible for causing viral hemorrhagic fever (VHF) in humans in South America (Junin, Guanarito, Sabia, Machupo, and Chapare viruses), West Africa (Lassa virus [LASV]), and South Africa (Lujo virus). Of these viruses, Lassa virus infection results in the highest levels of morbidity and mortality. Each year, there are up to 300,000 Lassa virus infections that result in approximately 5,000 deaths in areas of endemicity in West Africa (13, 14). While a majority of infected individuals recover, approximately 20% of the infected individuals develop a severe form of the disease affecting multiple organs. Although the virus infects many tissues, the resulting pathology is not severe enough to account for the cause of death (15). One consistent indicator of clinical prognosis is viral load (16). Those individuals with viremia levels of 8.5 log 10 PFU/ml usually succumb to the disease (17). Only one experimental vaccine exists for arenaviral VHF infection (Junin Candid 1 for Argentine hemorrhagic fever), and limited treatment options are available. Currently, ribavirin is the only therapeutic drug used in the treatment of Lassa fever, and it has proven efficacious, but only if administered early on during the course of infection (18). Unfortunately, Lassa fever is often misdiagnosed, and therefore, the window of opportunity for effective ribavirin usage can be missed (18, 19). Therefore, a better understanding of the pathogenesis of arenavirus infection may allow for the development of novel targeted therapeutics.

Because of the severity of the diseases they cause and the lack of effective vaccines and therapeutics, the arenaviruses that cause VHF in humans are classified as biosafety level 4 (BSL4) agents, which restricts research to those who have access to such specialized facilities. Pichinde virus (PICV) is a related arenavirus that does not cause disease in humans, but infection of guinea pigs with a strain that has been passaged 18 times (P18) through the spleens of guinea pigs (see Materials and Methods) produces a disease whose characteristics are similar to those of LASV infection of humans (20, 21). These characteristics include the correlation between the level of viremia with the severity of the disease, a similarity in the host tissue distribution of the virus, the development of a vascular leak syndrome which is often observed during terminal illness, the generalized immunosuppression, and, finally, the fact that the histopathological findings are not severe enough to explain the cause of death (15, 16, 20–29). This model thus provides a safe, economical, and informative alternative for studying VHF in a BSL2 setting.

An earlier passaged strain of PICV (P2) also causes disease in

Received 5 January 2013 **Accepted** 22 March 2013
Published ahead of print 3 April 2013
Address correspondence to Yuying Liang, liangy@umn.edu, or Hinh Ly, hly@umn.edu.

doi:10.1128/JVI.00044-13

guinea pigs. However, the disease is mild and is characterized by a brief febrile period and slight weight loss from which the animals quickly recover. This is in stark contrast to the disease course of P18 infection, in which the animals develop high fever and demonstrate dramatic weight loss until they reach a terminal point when the animals must be euthanized (21, 30, 31). This viral infection model provides us with the opportunity to examine what viral components are responsible for the phenotypic differences between these two strains and should help to elucidate which viral factors are involved in the pathogenesis of arenaviral VHF. It is remarkable that while the difference in phenotype between these two viral strains is dramatic, the viral sequences show limited diversity. In the L segment, the sequences encoding the Z proteins are completely identical, while the sequence for the L polymerase contains 5 amino acid differences between the two strains. In addition to the changes resulting in amino acid differences, there are also 11 silent mutations. There are 14 nucleotide changes in the GPC gene, 11 of which are silent and 3 of which are responsible for the amino acid differences between the two strains. Lastly, while there are a total of 19 nucleotide changes in the NP gene, only one of these results in an amino acid change between the viruses (32).

Our laboratory has previously described a reverse genetics system for both the P2 and P18 strains of PICV (30). For both strains, the L and S segments are expressed on separate plasmids, allowing for genetic manipulation of the viruses and generation of reassortant and recombinant mutant viruses. We present data herein that specify certain L protein residues of the P18 strain to be important for rapid virus replication in cell culture and *in vivo* and for the enhanced disease pathogenesis in infected animals.

MATERIALS AND METHODS

Viruses. The P2 and P18 PICV strains were adapted from Pichinde Munchique strain CoAn4763. This strain was passaged once in guinea pigs in Peter Jahrling's laboratory (USAMRIID). Subsequently, the virus was passaged again through the spleen of guinea pigs in Judy Aronson's laboratory (University of Texas Medical Branch [UTMB]) in order to produce the avirulent P2 strain. A virulent P15 virus, originating from Jahrling's original passage-adapted CoAn4763 adPIC virus, was obtained from Dorian Copenhaver (UTMB) and subsequently passaged 3 more times in inbred guinea pigs in Judy Aronson's laboratory to generate the virulent P18 virus (21).

Plasmids. L segment P2/P18 fragment swapping mutants were generated by using convenient restriction enzyme sites to cut and ligate fragments of P2 sequence from a plasmid expressing the P2 L segment into the corresponding location on a plasmid expressing the P18 L segment (previously described) (30). Point mutations were introduced into the P18L segment plasmid (30) via site-directed mutagenesis with a QuikChange mutagenesis kit (Stratagene). Mutagenesis was verified through DNA sequencing, and the fragments containing the intended point mutations were subcloned via convenient restriction enzymes into the unmanipulated P18 L segment plasmid.

Generation of recombinant viruses. BSRT7 cells constitutively expressing the T7 RNA polymerase were transfected in 6-well plates via Lipofectamine 2000 reagent (Invitrogen) with plasmids expressing the L and S genomic segments from the T7 promoter and terminator sequences. The medium was replaced at 4 h posttransfection, and supernatants were collected at 48 and 72 h. Viruses recovered in supernatants were plaque purified via plaque assay in Vero cells as previously described (30). Viruses from plaques were amplified by infection of BHK-21 cells cultured in 60-mm plates, and supernatants were collected at 72 h postinfection (hpi).

Plaque assay. Vero cells at near confluence were infected with 0.5 ml of serial dilutions of virus samples for 45 min at 37°C. After infection, viral samples were aspirated, and the cells were overlaid with fresh minimal essential medium (MEM) with 10% fetal bovine serum (FBS) and 0.5% agar. The cells were incubated for 4 days at 37°C. At day 4 postinfection, the cells were overlaid with MEM containing 10% FBS, 0.5% agar, and 0.02% neutral red dye. Plaques were enumerated on day 5 postinfection.

Animal experiments. Outbred male, 350- to 400-g, 4- to 5-week-old Dunkin Hartley guinea pigs were purchased from Charles River Laboratories and acclimatized for 5 to 7 days before initiation of the experimental studies. Animals were infected intraperitoneally (i.p.) with 10,000 PFU of virus. Body weights and rectal temperatures were monitored daily for 18 days. Beginning on day 7 postinfection, animals were supplemented with 40 ml/kg (of body weight) of lactated Ringer's solution plus 100 mg of ascorbic acid administered subcutaneously. Mortality was defined as animals having reached terminal points either when their body weight decreased by >30% compared to a nomogram or if the rectal temperature fell below 38°C in addition to body weight loss. According to our approved IACUC protocol, animals were allowed to be monitored for a maximum of 18 days after viral infection, at which time all surviving animals had to be euthanized. This is based on a comprehensive analysis of the disease course established in a large number of animals infected with P2 and P18 viruses (references 30 and 33 and our unpublished data).

In the current study, 19 animals were used to determine the attenuation levels of the fragment swapping mutants. Three animals were infected with the rS18L18(C2) viruses, and two separate groups of 8 animals each were infected with the rS18L18(D2) or rS18L18(A2) viruses. Groups of 6 animals each were used to test the single- and multiple-point mutant viruses. Statistical analyses of the survival curves were performed using the log-rank (Mantel-Cox) χ^2 test using GraphPad Prism 5 software. The statistical significance of the viral titers in the sera of the infected animals was analyzed using the Student *t* test.

Histopathology. Liver samples collected from animals infected with recombinant PICV were fixed using 4% formaldehyde, embedded in paraffin, sectioned, and stained with hematoxylin and eosin (H&E). The tissue slides were examined microscopically for histopathological changes by expert pathologists.

Viral growth curve analysis. Vero cells were seeded in 6-well plates at approximately 90% confluence. Cells were infected at a multiplicity of infection (MOI) of 0.01 for 45 min at 37°C. After infection, cells were washed with phosphate-buffered saline (PBS) before being supplemented with 2 ml of fresh medium. Supernatants were collected at various time points postinfection and assayed by plaque assay on Vero cells as previously described (30).

Real-time RT-PCR. Vero cells were infected with wild-type (WT) or mutant viruses at an MOI of 1. At 10 hpi, total cellular mRNA was collected using a Purelink RNA minikit (Ambion). On-column DNase digestion was performed using Purelink DNase according to the manufacturer's instructions (Ambion). Reverse transcription (RT) for generation of cDNAs was performed using the Superscript III kit (Invitrogen). Primer 5′-CGCACAGTGGATCCTAGGC-3′, which aligns to the 3′ untranslated region (UTR) of the S segment, was used to generate cDNAs of the viral genomic segment, while oligo(dT) was used to generate glyceraldehyde-3-phosphate dehydrogenase (GAPDH) cDNA for normalization purposes. Real-time RT-PCR was performed using SYBR green (Applied Biosciences); primers 5′-CAGGCTGAGACAAACTCTCAGTTC-3′ and 5′-GGACACAAGAGCACTGTTATCTGC-3′, each at 0.2 μM, were used for S segment detection, while primers 5′-GAAGGTGAAGGTCGGAGTC-3′ and 5′-CAAGCTTCCCGTTCTCAGCC-3′, each at 0.4 μM, were used to detect GAPDH. The cycling conditions included an initial incubation at 95°C for 10 min, followed by 40 cycles of 95°C for 15 s and 60°C for 1 min. Melting-curve analysis was performed from 60°C to 95°C at a rate of 0.3°C/s.

RESULTS

Generation of fragment swapping mutants between the P2 and P18 strains of the Pichinde virus L segment. In order to determine which segment(s) of the Pichinde virus might contain the

virulence factor(s), we previously generated and characterized a reassortant virus that expresses the L segment of the virulent P18 strain and the S segment of the avirulent P2 (S2L18) as well as the reverse reassortant virus that contains the L segment of P2 and the S segment of P18 (S18L2) (34). Both reassortant viruses were highly attenuated in infected guinea pigs, indicating that the virulence determinants were likely located on both segments of the viral genome. Analysis of these viruses indicated that the L segment was responsible for the higher rate of replication observed for the rP18 virus in tissue cultures, as the S2L18 reassortant virus showed a growth rate similar to that of the wild-type rP18 virus, whereas the S18L2 virus showed a growth curve similar to that of the rP2 virus (34). In Lassa virus-infected patients, high levels of viremia usually correlate with poor prognosis (16, 17). This implies that the rate of viral replication is an important factor in determining the degree of virulence and that amino acid substitutions are present in the L protein sequence that may be responsible for this phenotype.

In order to map the specific residue(s) that contributes to virulence within the L segment, we generated various fragment swapping mutants, effectively substituting different L fragments of the P2 sequence into the P18 genome (Fig. 1A). We reasoned that recombinant viruses with the substituted regions that contain virulence determinants would produce a loss-of-virulence phenotype in the infected animals.

The L segment contains 5 amino acid differences between the P2 and P18 strains: 4 amino acid substitutions are located in the C terminus, and another amino acid substitution is located in the N terminus of the L gene product. Multiple silent mutations are also found in this region of the viral genome, whereas the sequences encoding the Z protein are completely identical between the two strains of the virus (32). Based on unique restriction enzyme sites available along the L segment, we divided it into 4 fragments: D, C, B, and A. Since the B fragment is identical between the P2 and P18 strains, no fragment swapping mutant was generated for this region. With the other 3 fragments (D, C, and A), we introduced each fragment containing P2 sequence into the rP18 L segment. Specifically, the L18(A2) mutant contains the A fragment of P2 with an amino acid substitution at L protein sequence position 355 as well as 2 silent mutations, the L18(C2) mutant contains the C fragment of P2 with 5 silent mutations, and the L18(D2) mutant contains the D fragment of P2 with 4 amino acid differences at L protein sequence positions 1808, 1839, 1889, and 1906 as well as 3 silent mutations.

Virulence determinants of PICV P18 are localized to the C terminus of the L polymerase. In order to determine which fragment(s) of the L segment contains virulence determinants, we infected animals with the fragment swapping mutants (Fig. 1A) and monitored them for a loss of virulence. To do this, guinea pigs were infected intraperitoneally with 10,000 PFU of each recombinant virus, and body weight and temperature were monitored for 18 days. Three animals were infected with the rS18L18(C2) virus, and two separate groups of 8 animals each were infected with the rS18L18(D2) or rS18L18(A2) virus. Terminal points were defined as the point at which either an animal reached >30% weight loss compared to a nomogram or rectal temperature dropped below 38°C in combination with continuing weight loss. While the survival rate for rP18-infected animals was very low, all animals infected with rP2 virus survived. Results obtained with the recombinant viruses showed that both groups of guinea pigs that were

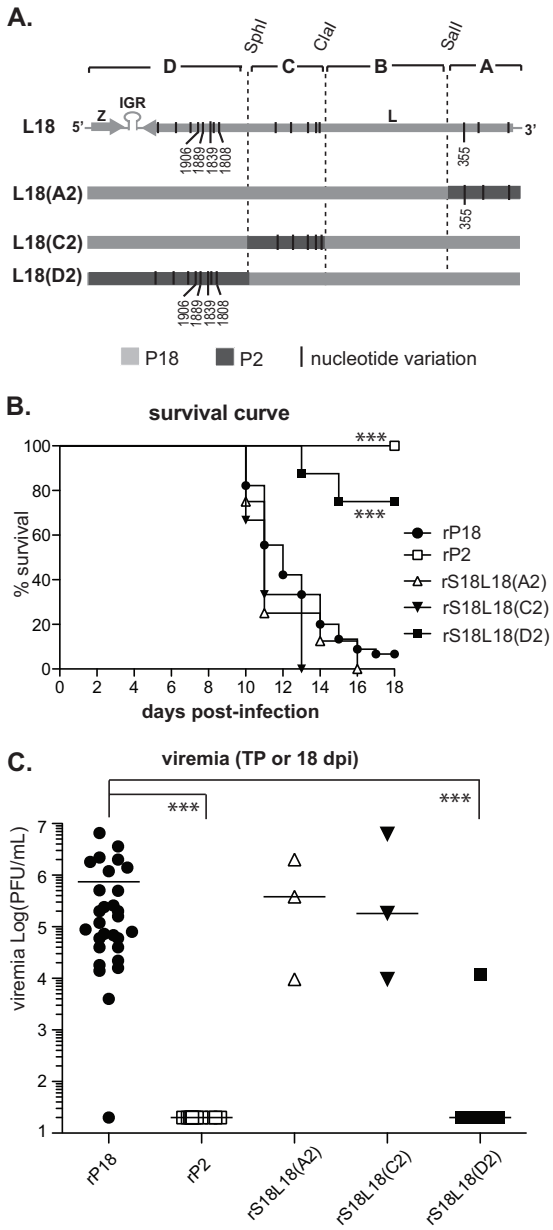

FIG 1 (A) Generation of recombinant P2/P18 L segment fragment swapping mutants. Based on available unique restriction enzyme sites, 3 fragment swapping mutants were generated, replacing a fragment of the P18 L segment with the corresponding sequence of the P2 genome. Sequence changes are highlighted in black, and changes that result in amino acid differences between the two strains are numbered. (B) Mortality of guinea pigs infected with L segment P2/P18 fragment swapping mutant recombinant viruses. The mortality rate was defined as the number of animals reaching terminal points (>30% weight loss compared to a nomogram or rectal temperature of <38°C in addition to a marked decrease in the weight of the animal) within the course of an 18-day infection. Numbers of infected animals are as follows: rP18, $n = 45$; rP2, $n = 24$; rS18L18(A2), $n = 8$; rS18L18(C2), $n = 3$; and rS18L18(D2), $n = 8$. (C) Viremia levels of guinea pigs infected with L segment P2/P18 fragment swapping mutant recombinant viruses. Serum samples collected at terminal points (TP) from animals infected with rS18L18(D2), rS18L18(C2), or rS18L18(A2) were analyzed by plaque assay to determine viral titers. Each data point represents one animal: rP18, $n = 29$; rP2, $n = 12$; rS18L18(A2), $n = 3$; rS18L18(C2), $n = 3$; and rS18L18(D2), $n = 6$. dpi, days postinfection. *, $P < 0.05$; **, $P < 0.01$; ***, $P < 0.001$.

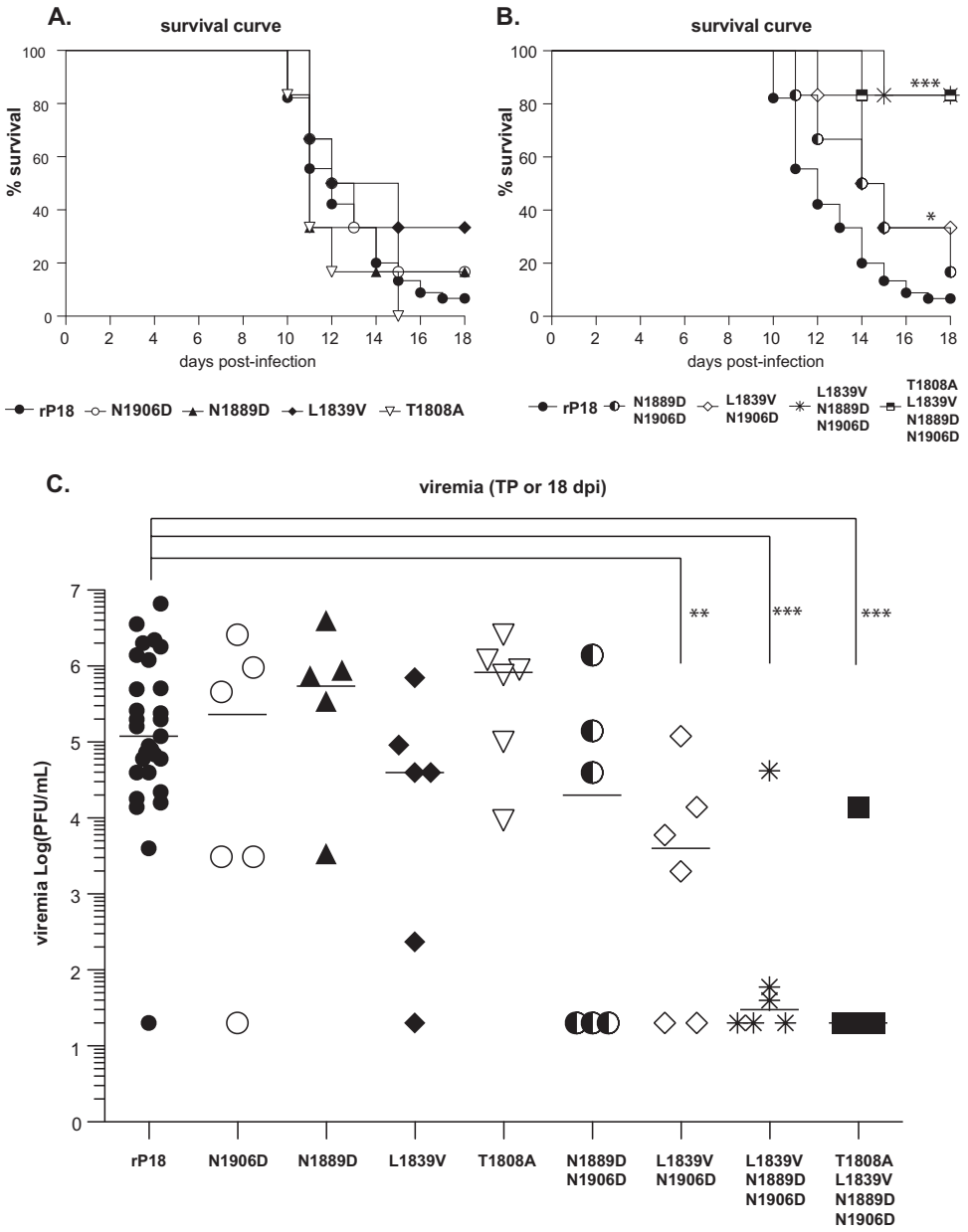

FIG 2 Mortality and viremia levels at terminal point of guinea pigs infected with single or combination point mutant viruses. (A) Mortality of animals infected with single point mutant viruses. Numbers of infected animals: rP18, $n = 45$, and recombinant mutant viruses, $n = 6$. (B) Mortality of animals infected with combination point mutant viruses. Numbers of infected animals: rP18, $n = 45$, and recombinant mutant viruses, $n = 6$. (C) Viremia levels at terminal points (or end of experiment for recovered animals) of guinea pigs infected with single and combination point mutant viruses. Each data point represents one animal: rP18, $n = 29$; N1889D mutant, $n = 5$; all other mutants, $n = 6$. *, $P < 0.05$; **, $P < 0.01$; ***, $P < 0.001$.

infected with rS18L18(A2) or with rS18L18(C2) showed 100% mortality (Fig. 1B). However, the group of animals infected with rS18L18(D2) showed a much higher (75%) rate of survival at day 18. The levels of viremia of the infected animals at terminal or experimental endpoints were determined by plaque assays. While sick animals maintained high viremia at time of death, the recovered animals had undetectable levels of virus (Fig. 1C).

Several point mutations in the C terminus of the L polymerase are involved in virus attenuation. Data from the fragment swapping experiment indicate that the D fragment of the L segment contains virulence determinants (Fig. 1). This fragment contains 4 amino acid substitutions at positions 1808, 1839, 1889, and 1906 as well as 3 silent mutations. We next wished to narrow down which of these sequence changes were responsible for the various phenotypes between the two strains of the virus. As the amino acid changes are the most likely candidates for disease attenuation, we decided to create point mutations at these residues by substituting the corresponding residue of the P2 sequence at each of these individual sites into the rP18 virus backbone. Consequently, recombinant N1906D, N1889D, L1839V, and T1808A viruses were generated and used to infect guinea pigs. Six animals per group were infected intraperitoneally with 10,000 PFU of each

TABLE 1 Macroscopic pathology observed in animals infected with combination point mutant viruses[a]

Combination point mutant virus	Animals with moderate to severe pathology	
	No./no. tested	%
N1906D/N1889D	4/6	67
N1906D/L1839V	4/6	67
N1906D/N1889D/L1839V	1/6	17
N1906D/N1889D/L1839V/T1808A	1/6	17

[a] Upon necropsy at terminal points, organs were visually inspected for signs of pathology. Organs in which moderate to severe pathology was noted included the liver and lungs. One animal in the N1906D/L1839Vvirus-infected group developed rectal prolapse.

of the recombinant viruses and monitored for 18 days for fever and body weight loss. While the L1839V virus seemed to be somewhat attenuated, the N1906D and N1889D viruses did not show any appreciable levels of attenuation (Fig. 2A). Notably, all animals infected with the T1808A recombinant virus died. Although the 1839V recombinant virus was somewhat attenuated, this virus did not reflect the dramatic loss of virulence that was noted in the fragment swapping mutant virus rS18L18(D2) (Fig. 1B).

As no single point mutation at the C terminus of the L polymerase could mirror the effect of introducing P2 sequence into the entire fragment D of the L segment, we reasoned that it is likely that a combination of the amino acid substitutions is required for the increased virulence of the P18 strain. We therefore generated several recombinant viruses carrying various combinations of these point mutations: N1906D/N1889D, N1906D/L1839V, N1906D/N1889D/L1839V, and N1906D/N1889D/L1839V/T1808A. While N1906D/L1839V virus was somewhat attenuated (Fig. 2B) in infected animals ($n = 6$), neither of the double mutants showed the dramatic attenuation noted with the fragment swapping mutant rS18L18(D2) (Fig. 1B). However, when all four residues were mutated to the corresponding residues of P2, the recombinant virus showed levels of attenuation that mirrored those of S18L18(D2) virus (Fig. 2B). Moreover, the triple mutant (N1906D/N1889D/L1839V) virus showed levels of attenuation similar to those of the quadruple mutant (N1906D/N1889D/L1839V/T1808A) virus and the fragment-swapped virus S18L18(D2), suggesting that residues N1889, L1839, and possibly N1906 located in the C-terminal domain of the viral polymerase work in concert with each other. In addition, 5 of the 6 animals infected with either the triple or quadruple mutant virus had extremely low or undetectable levels of viremia, while most of the animals infected with the single point mutant viruses or double mutant viruses retained high viral titers at terminal points (Fig. 2C). The degree of pathogenicity noted upon necropsy of infected animals reflected the mortality data (Table 1). Organs (liver, lung, small intestine, large intestine, and stomach) were visually inspected, and moderate gross pathology was defined as discoloration covering 50% of the individual organ, while severe pathology was determined by discoloration covering 75% of the organ or with signs of internal hemorrhaging. The most severe gross pathologies were noted in the liver and lungs. One animal in the N1906D/L1839V virus-infected group suffered rectal prolapse and was classified as having severe pathology. We therefore believe that certain residues in the L gene of the P18 strain are responsible for the intrinsic difference noted in the gross pathological changes in the organs of the infected animals.

H&E staining of liver tissue samples demonstrate that animals infected with the combination point mutant virus show reduced histopathology. In order to confirm visual inspection of the pathological differences between animal organs, H&E staining was performed on representative liver tissue samples from animals infected with the rP2, rP18, N1906D/N1889D, or N1906D/N1889D/L1839V/T1808A mutant virus. While the rP2-infected liver tissue sample looked relatively normal, the rP18-infected liver tissue showed severe pathology (Fig. 3). Large zones of necrosis were observed throughout the sample. Severe fatty change was noted throughout the tissue of the rP18-infected animals, along with acidophil bodies and ballooning degeneration. The pathology in the N1906D/N1889D liver sample was less severe but still showed ballooning degeneration and individual hepatocytes that appeared to be dying. While not as severe as in the rP18 sample, fatty changes were still noted. The histopathology from the liver samples of the N1906D/N1889D/L1839V/T1808A virus-infected animals showed hepatocytes that were largely healthy in appearance, while the presence of inflammatory cells within the portal veins was noted. Taken together, these histopathological results reflect the degrees of attenuation of some of the recombinant viruses noted in the mortality data shown in Fig. 2.

The increased virulence of PICV P18 is likely due in part to an increase in the rate of virus replication and efficiency of viral genomic RNA replication. As we have noted previously (30), the rP18 virus shows a higher rate of replication than its less pathogenic rP2 counterpart in cell culture. We therefore proceeded to analyze the growth curves of the recombinant mutant viruses used in the current study. To do this, Vero cells were infected with the different recombinant viruses at an MOI of 0.01 and virus supernatants were collected at 6, 12, 24, 36, 48, 60, 72, and 84 h postinfection. The single T1808A mutant virus appeared to replicate at a rate similar to that of the P18 virus (Fig. 4). The two recombinant N1906D/N1889D and N1906D/L1839D double mutant viruses showed replication rates that are higher than those of the triple and quadruple (N1906D/N1889D/L1839V and N1906D/N1889D/L1839V/T1808A) recombinant viruses, which remarkably almost overlapped with the growth curve produced by the rP2

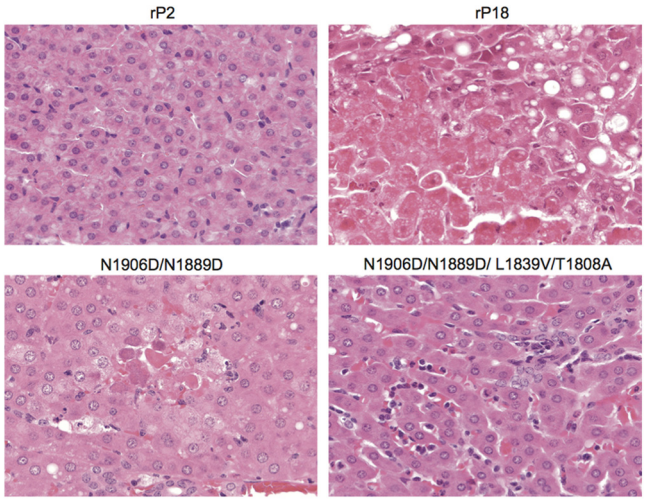

FIG 3 Liver pathology of infected animals. Shown is representative H&E staining of livers from guinea pigs infected with rP2, rP18, N1906D/N1889D, and N1906D/N1889D/L1839V/T1808A mutants.

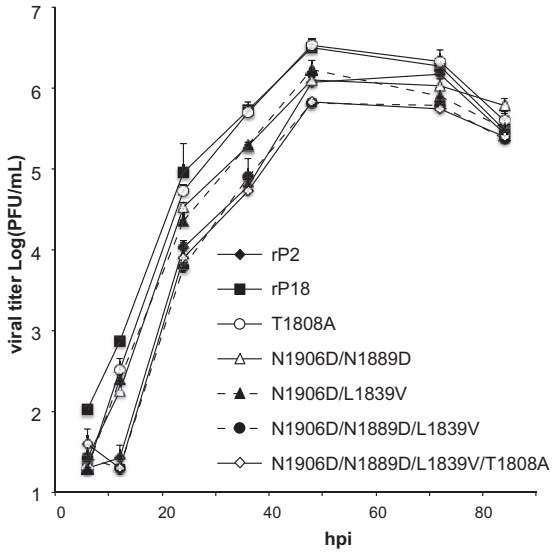

FIG 4 Growth curves of recombinant single or combination point mutant viruses. Vero cells were infected with various mutant viruses at an MOI of 0.01, and virus titers at various time points were determined by plaque assay.

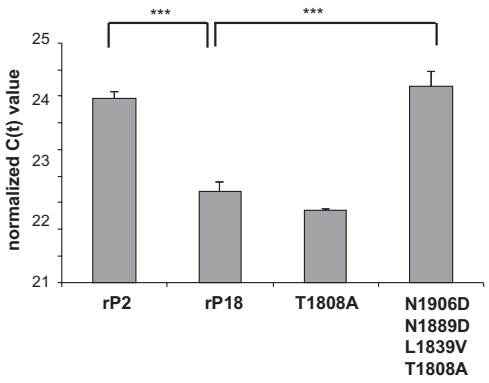

FIG 5 Real time RT-PCR analysis of genome replication in Vero cells infected with recombinant viruses. Vero cells were infected at an MOI of 1 with virus, RNA was collected, and RT was performed with a primer specific for the 3′ end of the genomic S segment. Real-time RT-PCR was performed with primers specific to the NP gene, and values were normalized with values for GAPDH transcripts. *, $P < 0.05$; **, $P < 0.01$; ***, $P < 0.001$.

virus (Fig. 4). These data suggest that the higher replication rates of some of these recombinant viruses may partly explain their more virulent nature in the infected animals.

In order to confirm that the lower growth rate of the recombinant virus exhibiting the combination of point mutations correlated with the lower rate of virus genome replication, we performed real-time RT-PCR to measure the amount of RNA genome replication occurring in the infected cells. To do this, Vero cells were infected with rP2, rP18, or the combination point mutant virus at an MOI of 1. RNA samples were collected at 10 hpi and assayed by real-time RT-PCR. The primer used for reverse transcription amplified only the viral genomic S segment, thus allowing for determination of the rate of virus genome replication. While the difference was not dramatic, the rP18 virus showed significantly higher levels of genome replication than rP2 (Fig. 5), which was reflected by the growth curves of these recombinant viruses in cell cultures (Fig. 4). Most notably, the quadruple mutant showed replication levels similar to that of the rP2 virus, suggestive of its attenuation level noted in the *in vivo* experiments (Fig. 2). Taken together, these data suggest that a modest increase in replicative efficiency of the P18 polymerase can partly contribute to the heightened degree of virulence in infected animals and that the three amino acid residues located at positions 1906, 1839, and 1889 of the L protein are critical for this phenotypic difference between the two PICV strains.

DISCUSSION

The mechanism by which arenaviruses cause severe hemorrhagic fever has long been speculated about but remains poorly understood. In this study, we have systematically analyzed natural sequence changes in the L segment of a virulent PICV arenavirus (P18) in order to elucidate which changes are responsible for the severe disease phenotype.

In LASV-infected patients, a strong correlation is observed between the levels of viral titer in the blood and clinical prognosis. Patients who recover from the illness are able to progressively reduce the levels of viremia, while fatally infected patients demonstrate uncontrolled viremia, eventually succumbing to the disease (16). Similarly, guinea pigs infected with virulent rP18 PICV virus maintain high viral titers in the blood until the animals reach terminal points and must be euthanized. Meanwhile, animals infected with the avirulent rP2 virus demonstrate undetectable levels of virus in the blood (Fig. 1C). However, rP2 viral replication is evidenced in the spleen, which is quickly eliminated (30). When the L polymerase mutant viruses were tested, they showed a similar trend; i.e., those animals with severe disease maintained high levels of viremia at the terminal points, whereas animals that were able to recover quickly controlled virus replication (Fig. 2C). Recently, a determinant of viral chronicity was mapped to position 1079 of the polymerase of lymphocytic choriomeningitis virus (LCMV). The clone 13 strain is able to establish a persistent infection, while the Armstrong strain causes acute infection which is quickly cleared. This single amino acid difference between the two strains was found to be responsible for the differential replicative capacities of the viral isolates *in vivo*, with the persistent strain showing higher replication rates. In addition to higher levels of viremia, this single mutation resulted in higher levels of RNA replication intracellularly as well as resulting in a generalized immunosuppression (35). Taken together, these data suggest that viral replicative capacity can serve as a good determinant of increased severity in arenavirus infection.

Through systematic mutagenesis, we were able to map virulence determinants to the C terminus of the PICV L polymerase that include a combination of N1906D, N1889D, and L1839V mutations, which produced a virus that was able to confer levels of attenuation similar to those observed for the fragment swapping rS18L18(D2) virus (Fig. 1 and 2). This suggests that these residues work in concert and are likely positioned in close proximity to one another in the tertiary structure of the protein that can modulate the polymerase catalytic function.

Structural information on negative-strand virus polymerases is currently scarce. While the crystal structures of the C-terminal domain of the PB2 subunit of the influenza virus polymerase (36) as well as a complex of the N terminus of influenza virus PB1 with the C terminus of PA (37) have been determined, the RNA-depen-

dent RNA polymerases (RdRps) of other negative-strand RNA viruses have proven difficult to crystallize. These proteins are extremely large (e.g., ~250 kDa for arenaviral L polymerase) and contain multiple functional domains. Sequence analysis has indicated that there are at least 4 conserved domains within the arenaviral L polymerase that are connected by highly variable linker regions (38). Domain III contains the RdRp, as evidenced by conserved motifs consistent with the RdRps of other negative-strand RNA viruses. Recently, the structure of the L1 domain of the LCMV polymerase, which consists of the first 196 amino acids, has successfully been solved and shown to fold into an endonuclease domain that is thought to be involved in the cap snatching process of viral transcription (39). However, the structures of the other domains of L polymerase remain elusive. Domains I and III of the Tacaribe virus L polymerase have been shown to be involved in binding the Z matrix protein, allowing Z to inhibit viral transcription (40). Many negative-strand viral polymerases, including the arenaviral RdRp, are known to oligomerize, which may be a requirement for transcription (41–44). Recently, studies have shown that the N terminus of the L protein may bind to the N terminus of another L subunit via domain I in a head-to-head conformation (38). Conversely, domains III and IV at the C terminus of one subunit may bind to the C terminus of another subunit (38). In addition, the N terminus of one subunit may also bind to the C terminus of another in a head-to-tail orientation (38). How these different conformations of oligomerization contribute to the function of the polymerase is yet to be understood. Currently, the exact residues involved in oligomerization of L are unknown. One possibility is that the residues identified in the current study as being important for the replicative differences between the two strains of PICV may affect the oligomerization state of the polymerase, although we have not formally tested this hypothesis. Also, the functions of domains II and IV of the polymerase remain unknown. Of note, the residues that we have identified in this study (N1906, N1889, and L1839) as critical for development of highly pathogenic PICV infection are located in domain IV. The sequence of this domain is unique and does not resemble any other known protein structures. While the residues identified in this study may potentially be involved in oligomerization of the polymerase, it is also possible that they might contribute to another unknown function(s) of domain IV. One such function that this domain could potentially contribute to is polymerase processivity.

The rP2 and rP18 viruses exhibit different rates of replication in tissue cultures, with the rP18 virus growing at a higher rate than the rP2 virus (Fig. 4) (30). Analyses of reassortant viruses have determined that the L segment is responsible for the observed differences in growth rate, as the sequences of the Z protein are identical between the two strains. We confirmed by real-time RT-PCR that the P18 virus is more efficient at catalyzing viral genomic RNA replication than its P2 counterpart (Fig. 5). We have introduced various natural sequence changes into the P18 polymerase and tested the effects of the mutations on viral genome replication. Once again, while individual mutations showed little effect on the rate of genome replication, a combination of the point mutations in the C terminus of L reduced the levels of RNA replication, more closely resembling the levels seen in the P2 virus. Because these mutations in domain IV affected the efficiency of the polymerase function, we propose that this domain may be involved in determining the rate of polymerase activity. Taken together, these data suggest that rapid virus replication as a result of enhanced polymerase activity plays an important role in determining the degree of virulence in arenavirus-induced VHFs. Other viral polymerases, such as that of influenza virus, have also been shown to contribute to disease virulence (45–47).

While we have shown in the current study that sequence variations in arenaviral L polymerase play an important role in determining the degree of virulence, it is important to note that the pathogenic nature of arenavirus VHFs may involve other factors. For example, reassortant analysis of P2 and P18 PICVs has indicated that additional viral virulence determinants may also be localized to the GPC and NP genes present on the S segment of the viral genome (34). Therefore, we do not expect that introduction of the critical virulence-associated residues in the L gene from the P18 into the P2 virus alone would result in a complete recovery of the P18 phenotype. The binding affinity of the viral glycoprotein (GPC) to its receptor has been implicated as an important factor for viral pathogenesis (48, 49). While the receptor used by PICV is currently unknown, several New World arenaviruses that cause hemorrhagic fevers are known to use the human transferrin receptor 1 (TfR1) as their cellular receptor (50, 51), while the nonpathogenic Tacaribe and Amapari viruses use TfR1 orthologs but cannot gain entry into cells via the human TfR1 (52). Old World arenaviruses such as LASV utilize alpha-dystroglycan (αDG) as their cellular receptor (48, 53). LCMV clone 13, which causes chronic infection of mice, has a high affinity for αDG, as it is able to displace laminin, the natural cellular ligand for αDG (48). Meanwhile, LCMV Armstrong, which causes an acute infection, is unable to displace laminin (48, 49). This evidence indicates the contribution of the GPC gene in arenavirus pathogenicity. Recent data from our laboratory and others have indicated that the nucleoprotein (NP) gene, which is contained in the S segment, is involved in suppressing type I interferon (IFN) (10–12). Arenaviral hemorrhagic fever has been shown to be associated with a generalized immunosuppression, thereby enhancing viral replication and disease pathogenesis (54–60), and NP may contribute to this mechanism of host innate immune suppression. While most viral proteins that inhibit IFN production do so by inhibiting steps in the signal transduction pathway, the arenaviral NP functions in a unique manner. The C terminus of the protein contains an exoribunuclease domain, which has been shown to be responsible for the IFN inhibition function of the protein by possibly degrading RNA substrates that can be recognized as viral pathogen-associated molecular patterns (PAMPs) by the host (12, 61, 62). While the pathogenesis of severe arenaviral infections does appear to be multigenic, we show here that differences in the viral L polymerase gene alone can greatly influence the degree of disease pathogenesis *in vivo*. Unique regions of the polymerase identified in this study to be involved in viral replication efficiency may provide novel targets for effective antiviral development and therapy.

ACKNOWLEDGMENTS

We thank J. Aronson (University of Texas Medical Branch) for providing P2 and P18 viruses and T. G. Parslow and V. Adsay for providing expert consultation on liver pathology.

This work was supported by NIH grants R01AI083409 to Y.L. and R01AI093580 and R56AI091805 to H.L.

REFERENCES

1. **Buchmeier M, Bowen M, Peters C.** 2001. Arenaviridae: the viruses and their replication, p 1635–1668. *In* Knipe DM, Howley PM, Griffin DE,

Lamb RA, Martin MA, Roizman B, Straus SE (ed), Fields virology, 4th ed, **vol 2**. Lippincott Williams & Wilkins, Philadelphia, PA.
2. **Wilson S, Clegg J.** 1991. Sequence analysis of the S RNA of the African arenavirus Mopeia: an unusual secondary structure feature in the intergenic region. Virology **180**:543–552.
3. **Hass M, Westerkofsky M, Müller S, Becker-Ziaja B, Busch C, Günther S.** 2006. Mutational analysis of the Lassa virus promoter. J. Virol. **80**: 12414–12419.
4. **Lee KJ, de la Torre JC.** 2002. Reverse genetics of arenaviruses. Curr. Top. Microbiol. Immunol. **262**:175–193.
5. **Perez M, de la Torre JC.** 2003. Characterization of the genomic promoter of the prototypic arenavirus lymphocytic choriomeningitis virus. J. Virol. **77**:1184–1194.
6. **Hass M, Gölnitz U, Müller S, Becker-Ziaja B, Günther S.** 2004. Replicon system for Lassa virus. J. Virol. **78**:13793–13803.
7. **Lee KJ, Novella IS, Teng MN, Oldstone MBA, de la Torre JC.** 2000. NP and L proteins of lymphocytic choriomeningitis virus (LCMV) are sufficient for efficient transcription and replication of LCMV genomic RNA analogs. J. Virol. **74**:3470–3477.
8. **López N, Jácamo R,Franze-Fernández MT.** 2001. Transcription and RNA replication of Tacaribe virus genome and antigenome analogs require N and L proteins: Z protein is an inhibitor of these processes. J. Virol. **75**:12241–12251.
9. **Martínez-Sobrido L, Emonet S, Giannakas P, Cubitt B, García-Sastre A, de la Torre JC.** 2009. Identification of amino acid residues critical for the anti-interferon activity of the nucleoprotein of the prototypic arenavirus lymphocytic choriomeningitis virus. J. Virol. **83**:11330–11340.
10. **Martínez-Sobrido L, Giannakas P, Cubitt B, García-Sastre A, de la Torre JC.** 2007. Differential inhibition of type I interferon induction by arenavirus nucleoproteins. J. Virol. **81**:12696–12703.
11. **Martínez-Sobrido L, Zúñiga EI, Rosario D, García-Sastre A, de la Torre JC.** 2006. Inhibition of the type I interferon response by the nucleoprotein of the prototypic arenavirus lymphocytic choriomeningitis virus. J. Virol. **80**:9192–9199.
12. **Qi X, Lan S, Wang W, Schelde LM, Dong H, Wallat GD, Ly H, Liang Y, Dong C.** 2010. Cap binding and immune evasion revealed by Lassa nucleoprotein structure. Nature **468**:779–783.
13. **Günther S, Lenz O.** 2004. Lassa virus. Crit. Rev. Clin. Lab. Sci. **41**:339–390.
14. **McCormick J, Webb P, Krebs J, Johnson K, Smith E.** 1987. A prospective study of the epidemiology and ecology of Lassa fever. J. Infect. Dis. **155**:437–444.
15. **Walker D, McCormick J, Johnson K, Webb P, Komba-Kono G, Elliott L, Gardner J.** 1982. Pathologic and virologic study of fatal Lassa fever in man. Am. J. Pathol. **107**:349–356.
16. **Johnson KM, McCormick JB, Webb PA, Smith ES, Elliott LH, King IJ.** 1987. Clinical virology of Lassa fever in hospitalized patients. J. Infect. Dis. **155**:456–464.
17. **Oldstone MBA, Campbell KP.** 2011. Decoding arenavirus pathogenesis: essential roles for alpha-dystroglycan-virus interactions and the immune response. Virology **411**:170–179.
18. **McCormick JB, King IJ, Webb PA, Scribner CL, Craven RB, Johnson KM, Elliott LH, Belmont-Williams R.** 1986. Lassa fever. N. Engl. J. Med. **314**:20–26.
19. **McCormick JB, King IJ, Webb PA, Johnson KM, O'Sullivan R, Smith ES, Trippel S, Tong TC.** 1987. A case-control study of the clinical diagnosis and course of Lassa fever. J. Infect. Dis. **155**:445–455.
20. **Aronson J, Herzog N, Jerrells T.** 1994. Pathological and virological features of arenavirus disease in guinea pigs. Comparison of two Pichinde virus strains. Am. J. Pathol. **145**:228–235.
21. **Jahrling PB, Hesse RA, Rhoderick JB, Elwell MA, Moe JB.** 1981. Pathogenesis of a Pichinde virus strain adapted to produce lethal infections in guinea pigs. Infect. Immun. **32**:872–880.
22. **Aronson J, Herzog N, Jerrells T.** 1995. Tumor necrosis factor and the pathogenesis of Pichinde virus infection in guinea pigs. Am. J. Trop. Med. Hyg. **52**:262–269.
23. **Bowick GC, Fennewald SM, Elsom BL, Aronson JF, Luxon BA, Gorenstein DG, Herzog NK.** 2006. Differential signaling networks induced by mild and lethal hemorrhagic fever virus infections. J. Virol. **80**:10248–10252.
24. **Connolly BM, Jenson AB, Peters CJ, Geyer SJ, Barth JF, McPherson RA.** 1993. Pathogenesis of Pichinde virus infection in strain 13 guinea pigs: an immunocytochemical, virologic, and clinical chemistry study. Am. J. Trop. Med. Hyg. **49**:10–24.
25. **Fennewald SM, Aronson JF, Zhang L, Herzog NK.** 2002. Alterations in NF-κB and RBP-J.κ by arenavirus infection of macrophages in vitro and in vivo. J. Virol. **76**:1154–1162.
26. **Katz MA, Starr JF.** 1990. Pichinde virus infection in strain 13 guinea pigs reduces intestinal protein reflection coefficient with compensation. J. Infect. Dis. **162**:1304–1308.
27. **Lucia HL, Coppenhaver DH, Harrison RL, Baron S.** 1990. The effect of an arenavirus infection on liver morphology and function. Am. J. Trop. Med. Hyg. **43**:93–98.
28. **Peters C, Liu C, Anderson G, Morrill J, Jahrling P.** 1989. Pathogenesis of viral hemorrhagic fevers: Rift Valley fever and Lassa fever contrasted. Rev. Infect. Dis. **11**(Suppl 4):S743–S749.
29. **Qian C, Jahrling PB, Peters C, Liu C.** 1994. Cardiovascular and pulmonary responses to Pichinde virus infection in strain 13 guinea pigs. Lab. Anim. Sci. **44**:600–607.
30. **Lan S, McLay Schelde L, Wang J, Kumar N, Ly H, Liang Y.** 2009. Development of infectious clones for virulent and avirulent Pichinde viruses: a model virus to study arenavirus-induced hemorrhagic fevers. J. Virol. **83**:6357–6362.
31. **Zhang L, Marriott K, Aronson JF.** 1999. Sequence analysis of the small RNA segment of guinea pig-passaged Pichinde virus variants. Am. J. Trop. Med. Hyg. **61**:220–225.
32. **Lan S, McLay L, Aronson J, Ly H, Liang Y.** 2008. Genome comparison of virulent and avirulent strains of the Pichinde arenavirus. Arch. Virol. **153**:1241–1250.
33. **Zhang L, Marriott KA, Harnish DG, Aronson JF.** 2001. Reassortant analysis of guinea pig virulence of Pichinde virus variants. Virology **290**: 30–38.
34. **Liang Y, Lan S, Ly H.** 2009. Molecular determinants of Pichinde virus infection of guinea pigs—a small animal model system for arenaviral hemorrhagic fevers. Ann. N. Y. Acad. Sci. **1171**:E65–E74. doi:10.1111/j.1749-6632.2009.05051.x.
35. **Bergthaler A, Flatz L, Hegazy AN, Johnson S, Horvath E, Löhning M, Pinschewer DD.** 2010. Viral replicative capacity is the primary determinant of lymphocytic choriomeningitis virus persistence and immunosuppression. Proc. Natl. Acad. Sci. U. S. A. **107**:21641–21646.
36. **Tarendeau F, Boudet J, Guilligay D, Mas PJ, Bougault CM, Boulo S, Baudin F, Ruigrok RWH, Daigle N, Ellenberg J, Cusack S, Simorre J-P, Hart DJ.** 2007. Structure and nuclear import function of the C-terminal domain of influenza virus polymerase PB2 subunit. Nat. Struct. Mol. Biol. **14**:229–233.
37. **He X, Zhou J, Bartlam M, Zhang R, Ma J, Lou Z, Li X, Li J, Joachimiak A, Zeng Z, Ge R, Rao Z, Liu Y.** 2008. Crystal structure of the polymerase PAC-PB1N complex from an avian influenza H5N1 virus. Nature **454**: 1123–1126.
38. **Brunotte L, Lelke M, Hass M, Kleinsteuber K, Becker-Ziaja B, Günther S.** 2011. Domain structure of Lassa virus L protein. J. Virol. **85**:324–333.
39. **Morin B, Coutard B, Lelke M, Ferron F, Kerber R, Jamal S, Frangeul A, Baronti C, Charrel R, de Lamballerie X, Vonrhein C, Lescar J, Bricogne G, Günther S, Canard B.** 2010. The N-terminal domain of the arenavirus L protein is an RNA endonuclease essential in mRNA transcription. PLoS Pathog. **6**:e1001038. doi:10.1371/journal.ppat.1001038.
40. **Wilda M, Lopez N, Casabona JC, Franze-Fernandez MT.** 2008. Mapping of the Tacaribe arenavirus Z-protein binding sites on the L protein identified both amino acids within the putative polymerase domain and a region at the N terminus of L that are critically involved in binding. J. Virol. **82**:11454–11460.
41. **Sánchez AB, de la Torre JC.** 2005. Genetic and biochemical evidence for an oligomeric structure of the functional L polymerase of the prototypic arenavirus lymphocytic choriomeningitis virus. J. Virol. **79**:7262–7268.
42. **Smallwood S, Çevik B, Moyer SA.** 2002. Intragenic complementation and oligomerization of the L subunit of the Sendai virus RNA polymerase. Virology **304**:235–245.
43. **Smallwood S, Moyer SA.** 2004. The L polymerase protein of parainfluenza virus 3 forms an oligomer and can interact with the heterologous Sendai virus L, P and C proteins. Virology **318**:439–450.
44. **Zamoto-Niikura A, Terasaki K, Ikegami T, Peters CJ, Makino S.** 2009. Rift Valley fever virus L protein forms a biologically active oligomer. J. Virol. **83**:12779–12789.
45. **Ping J, Dankar SK, Forbes NE, Keleta L, Zhou Y, Tyler S, Brown EG.** 2010. PB2 and hemagglutinin mutations are major determinants of host

range and virulence in mouse-adapted influenza A virus. J. Virol. **84**: 10606–10618.
46. **Tada T, Suzuki K, Sakurai Y, Kubo M, Okada H, Itoh T, Tsukamoto K.** 2011. NP body domain and PB2 contribute to increased virulence of H5N1 highly pathogenic avian influenza viruses in chickens. J. Virol. **85**: 1834–1846.
47. **Xu L, Bao L, Zhou J, Wang D, Deng W, Lv Q, Ma Y, Li F, Sun H, Zhan L, Zhu H, Ma C, Shu Y, Qin C.** 2011. Genomic polymorphism of the pandemic A (H1N1) influenza viruses correlates with viral replication, virulence, and pathogenicity *in vitro* and *in vivo*. PLoS One **6**:e20698. doi: 10.1371/journal.pone.0020698.
48. **Kunz S, Sevilla N, McGavern DB, Campbell KP, Oldstone MBA.** 2001. Molecular analysis of the interaction of LCMV with its cellular receptor α-dystroglycan. J. Cell Biol. **155**:301–310.
49. **Smelt SC, Borrow P, Kunz S, Cao W, Tishon A, Lewicki H, Campbell KP, Oldstone MBA.** 2001. Differences in affinity of binding of lymphocytic choriomeningitis virus strains to the cellular receptor α-dystroglycan correlate with viral tropism and disease kinetics. J. Virol. **75**:448–457.
50. **Flanagan ML, Oldenburg J, Reignier T, Holt N, Hamilton GA, Martin VK, Cannon PM.** 2008. New World clade B arenaviruses can use transferrin receptor 1 (TfR1)-dependent and -independent entry pathways, and glycoproteins from human pathogenic strains are associated with the use of TfR1. J. Virol. **82**:938–948.
51. **Radoshitzky SR, Abraham J, Spiropoulou CF, Kuhn JH, Nguyen D, Li W, Nagel J, Schmidt PJ, Nunberg JH, Andrews NC, Farzan M, Choe H.** 2007. Transferrin receptor 1 is a cellular receptor for New World haemorrhagic fever arenaviruses. Nature **446**:92–96.
52. **Abraham J, Kwong JA, Albariño CG, Lu JG, Radoshitzky SR, Salazar-Bravo J, Farzan M, Spiropoulou CF, Choe H.** 2009. Host-species transferrin receptor 1 orthologs are cellular receptors for nonpathogenic New World clade B arenaviruses. PLoS Pathog. **5**:e1000358. doi:10.1371/journal.ppat.1000358.
53. **Cao W, Henry M, Borrow P, Yamada H, Elder J, Ravkov E, Nichol S, Compans R, Campbell K, Oldstone M.** 1998. Identification of alpha-dystroglycan as a receptor for lymphocytic choriomeningitis virus and Lassa fever virus. Science **282**:2079–2081.
54. **Baize S, Kaplon J, Faure C, Pannetier D, Georges-Courbot M-C, Deubel V.** 2004. Lassa virus infection of human dendritic cells and macrophages is productive but fails to activate cells. J. Immunol. **172**:2861–2869.
55. **Baize S, Marianneau P, Loth P, Reynard S, Journeaux A, Chevallier M, Tordo N, Deubel V, Contamin H.** 2009. Early and strong immune responses are associated with control of viral replication and recovery in Lassa virus-infected cynomolgus monkeys. J. Virol. **83**:5890–5903.
56. **Edington G, White H.** 1972. The pathology of Lassa fever. Trans. R. Soc. Trop. Med. Hyg. **66**:381–389.
57. **Fisher-Hoch S, McCormick J, Sasso D, Craven R.** 1988. Hematologic dysfunction in Lassa fever. J. Med. Virol. **26**:127–135.
58. **Mahanty S, Hutchinson K, Agarwal S, McRae M, Rollin PE, Pulendran B.** 2003. Cutting edge: impairment of dendritic cells and adaptive immunity by Ebola and Lassa viruses. J. Immunol. **170**:2797–2801.
59. **McCormick J, Fisher-Hoch S.** 2002. Lassa fever. Curr. Top. Microbiol. Immunol. **262**:75–109.
60. **Müller S, Geffers R, Günther S.** 2007. Analysis of gene expression in Lassa virus-infected HuH-7 cells. J. Gen. Virol. **88**:1568–1575.
61. **Brunotte L, Kerber R, Shang W, Hauer F, Hass M, Gabriel M, Lelke M, Busch C, Stark H, Svergun DI, Betzel C, Perbandt M, Günther S.** 2011. Structure of the Lassa virus nucleoprotein revealed by X-ray crystallography, small-angle X-ray scattering, and electron microscopy. J. Biol. Chem. **286**:38748–38756.
62. **Hastie KM, Kimberlin CR, Zandonatti MA, MacRae IJ, Saphire EO.** 2011. Structure of the Lassa virus nucleoprotein reveals a dsRNA-specific 3′ to 5′ exonuclease activity essential for immune suppression. Proc. Natl. Acad. Sci. U. S. A. **108**:2396–2401.